Volume 6
Number 17
7 September 2024
Pages 4263–4494

Nanoscale Advances

rsc.li/nanoscale-advances

ISSN 2516-0230

ROYAL SOCIETY OF CHEMISTRY

PAPER

Seunghyun Rhee, Jeongkyun Roh *et al.*
Utilizing a compact diamino-based ligand as a charge balancer in quantum dot light-emitting diodes

NCNST

Nanoscale Advances

ROYAL SOCIETY OF CHEMISTRY

PAPER

View Article Online
View Journal | View Issue

Cite this: *Nanoscale Adv.*, 2024, **6**, 4369

Utilizing a compact diamino-based ligand as a charge balancer in quantum dot light-emitting diodes†

Minseok Choi,[a] Woon Ho Jung,[b] Jaeyeop Lee,[a] Yeyun Bae,[a] Kyoungeun Lee,[a] Jiyoon Oh,[a] Jaehoon Lim,[bcd] Seunghyun Rhee*[e] and Jeongkyun Roh*[a]

Charge imbalance within the emissive layer (EML) has been identified as a major obstacle to achieving high-performance quantum dot light-emitting diodes (QD-LEDs). To address this issue, we propose the use of a compact diamino-based ligand as a universal approach to improve the charge balance within the QD EML. Specifically, we treat QDs symmetrically with 1,4-diaminobutane (DAB) on both the bottom and top sides. This treatment simultaneously modulates the injection properties of electrons and holes, effectively suppressing electron injection into QDs while facilitating hole injection. As a result, QD-LEDs with symmetrical DAB treatment exhibit a 1.5-fold increase in external quantum efficiency and a remarkable 4.5-fold increase in device lifetime. These results highlight the role of the compact diamine-based ligands as highly efficient charge balancers to realize high-performance and highly stable QD-LEDs.

Received 25th April 2024
Accepted 15th June 2024

DOI: 10.1039/d4na00348a

rsc.li/nanoscale-advances

1. Introduction

Colloidal quantum dots (QDs) have attracted attention due to their attractive properties for next-generation displays[1–3] such as high photoluminescence quantum yield,[4,5] narrow full-width half-maximum (FWHM),[6,7] and tunable emission wavelengths.[8,9] Numerous studies have aimed at integrating QDs into electrically pumpable structures, with a focus on realizing self-emitting displays through the development of QD-based light-emitting diodes (QD-LEDs). Significant progress in the improvement of luminescent QDs and the optimization of device architecture has led to a remarkable increase in the external quantum efficiency (EQE) of QD-LEDs, exceeding the theoretical limit of 20%. However, the commercialization of QD-LEDs has been hindered by the stability issue.

One of the main factors contributing to the limited stability of QD-LEDs is the occurrence of charge imbalance within the QD emissive layer (EML) during operation. In QD-LEDs, QDs are surrounded by charge transport layers (CTLs), and differences in carrier injection rates from CTLs often lead to QD charging, thereby inducing non-radiative Auger recombination.[10] This detrimental process significantly degrades the luminescence efficiency and overall lifetime of QD-LEDs. The typical configuration of CTLs consists of a zinc oxide (ZnO)-based inorganic electron transport layer (ETL)[11,12] and an organic hole transport layer (HTL), where a charge imbalance arises due to the faster injection rate of electrons compared to holes.[13–15] This discrepancy is attributed to the higher electron mobility of ZnO-based ETLs compared to that of organic HTLs.[16] In addition, the favorable band alignment between ZnO and QDs can facilitate to the spontaneous injection of electrons into QDs, further exacerbating the charge balance problem.

To address this challenge, numerous approaches have been explored to suppress electron injection and improve charge balance. These approaches involve the insertion of insulating layers,[17,18] and the reduction of ZnO conductivity through doping.[19,20] Alternative strategies have focused on enhancing hole injection by employing cascaded HTLs, implementing interfacial dipoles to reduce hole injection barriers,[20–22] and increasing hole mobility in organic HTLs through doping.[23] Ideally, simultaneous modification of both electron and hole injection properties is crucial, yet research in this area has been limited. Our group has recently demonstrated the successful enhancement of charge balance in quasi-type II QD-based LEDs by using 1,12-diaminododecane (DAD) ligand, which acts as a charge balancer for both holes and electrons.[24] The DAD treatment on the electron injecting side suppresses electron injection, while its application on the hole injecting side

[a]*Dept. of Electrical Engineering, Pusan National University, Busan 46241, Republic of Korea. E-mail: jkroh@pusan.ac.kr*

[b]*Dept. of Energy Science and Center for Artificial Atoms, Sungkyunkwan University, Suwon, Gyeonggi-do 16419, Republic of Korea*

[c]*SKKU Institute of Energy Science and Technology (SIEST), Sungkyunkwan University, Suwon, Gyeonggi-do 16419, Republic of Korea*

[d]*Department of Future Energy Engineering (DFEE), Sungkyunkwan University, Suwon, Gyeonggi-do 16419, Republic of Korea*

[e]*Advanced Materials Division, Korea Research Institute of Chemical Technology (KRICT), Daejeon, 34114, Republic of Korea. E-mail: rheejoe@krict.re.kr*

† Electronic supplementary information (ESI) available. See DOI: https://doi.org/10.1039/d4na00348a

enhances hole injection by inducing an interfacial dipole. As a result, the use of DAD as a charge balancer led to a significant improvement in external quantum efficiency (EQE) and maximum luminance by 8 and 10 times, respectively. Despite the effective modulation of both hole and electron injection rates, its effectiveness was diminished when employing type I QDs. Therefore, a more universal method suitable for different types of QDs should be developed.

In this study, we present 1,4-diaminobutane (DAB) as a compact charge balancer capable of effectively modulating charge injection rates in type I QD-based LEDs. Due to its short chain length, DAB treatment induces sufficient dipoles at the interfaces without affecting the morphology, thereby modulating the charge injection rates in type I QD-based LEDs. Symmetrical application of DAB to QDs modifies the energy landscape of QD-LEDs in a way that suppresses electron injection and enhances hole injection. As a result, QD-LEDs with DAB treatment demonstrates an enhancement in maximum EQE and luminance by a factor of 1.5. Furthermore, the improved charge balance achieved by DAB treatment leads to an increased operating lifetime (T_{60} lifetime under 900 nit increased from 1.22 h to 5.44 h). In addition, we validated its universality across different structures (*i.e.*, conventional or inverted) of QD-LEDs.

2. Experimental section

2.1 Chemicals for synthesis and device fabrication

Tris(4-carbazoyl-9-ylphenyl) amine (TCTA, ≥97%), 1,4-diaminobutane (DAB, ≥99%), ethanol (≥99.5%), zinc acetate dihydrate (≥99.0%), butanolamine (≥99.5%),and octane (≥99%) were purchased from Sigma-Aldrich. PEDOT:PSS was purchased from Heraeus Electronic Materials Division. Molybdenum(VI) oxide (MoO_3, 99.995%) and aluminium (Al) pellets were purchased from Taewon Scientific Co. IPA (≥99.9%), potassium hydroxide (KOH), acetone (≥99.7%) and methanol (≥99.9%) were purchased from Samchun Chemicals. TFB was purchased from OSM and the patterned ITO substrates were purchased from AMG. All chemicals were used as received without any purification.

2.2 Synthesis of ZnO nanoparticles

KOH (2.5 g) was sonicated in a methanol solution for 30 min and a solution containing 5 g of zinc acetate dihydrate, 200 mL of methanol, and 0.8 mL of deionized water was loaded into a three-neck flask and heated to 60 °C for 30 min under 900 rpm stirring. The KOH solution was then added to the three-neck flask containing the zinc acetate dihydrate solution to initiate a chemical reaction, which proceeded for 2.5 h. Following this reaction, the solution containing ZnO nanoparticles were centrifuged and purified twice using methanol. The purified ZnO nanoparticles were subsequently treated with butylamine ligands and dissolved in butanol for further use.

2.3 Synthesis of QDs

Zinc acetate (99.999%) selenium powder (200 mesh, 99.999) and sulfur powder (99.98%) were purchased from Sigma-Aldrich. Oleic acid (OA, 90%), trioctylphosphine (TOP, 97%), 1-octadecene (ODE, 99%), cadmium oxide (CdO, 99.95%) myristic acid (My, 99%) and 1-dodecanethiol (DDT, 98%) were purchased from Alfa Aesar. All chemicals were used as received without further purification.

The method reported by Lisa zur Borg *et al.*[25] was adopted with slight modifications for the synthesis of red-emitting CdSe/CdS/CdZnS QDs. Zinc oleate ($Zn(OA)_2$), cadmium oleate ($Cd(OA)_2$), TOP-Se and TOP-S stock solutions were prepared prior to QD synthesis under inert atmosphere conditions. Specifically, 0.5 M of $Zn(OA)_2$ was prepared by reacting 20 mmol of zinc acetate, 20 mL of OA in 20 mL of 1-octadecane at 120 °C under vacuum (<500 mTorr) for 30 min. Similarly, 0.5 M $Cd(OA)_2$ was synthesized by reacting 20 mmol of CdO with 20 mL of OA in 20 mL of ODE at 270 °C. Both stock solutions were maintained at 100 °C to prevent solidification. Additionally, 2 M of TOPSe and 2 M of TOPS solutions were prepared by mixing 20 mmol of selenium or sulfur with 10 mL of trioctylphosphine (TOP). All stock solutions were stored under an inert atmosphere.

To prepare the red-emitting CdSe cores capped with a CdS shell, $Cd(My)_2$ was prepared using 1 mmol of CdO, 3 mmol of My, and 15 mL of ODE with temperature raised to 270 °C followed by the rapid injection of 0.5 mmol of TOPSe. Subsequently, the temperature was raised to 300 °C, and 1.5 mmol of dodecanethiol (DDT) and 1 mmol of $Zn(OA)_2$ were added dropwise. The reaction was maintained for 30 min. To overcoat the CdZnS shell, 2 mmol of $Zn(OA)_2$ and 3 mmol of TOPS were injected, followed by the slow addition of 2 mmol of $Cd(OA)_2$ to prevent nucleation of CdS. After 9 min, 3 mmol $Zn(OA)_2$, 4 mmol of TOPS, and 1.5 mmol of $Cd(OA)_2$ were added in a similar manner. The reaction was rapidly quenched to room temperature after 5 min. The crude solution underwent purification through four cycles of precipitation (using acetone) and redispersion (in toluene). The final product was dispersed in octane for the fabrication of QD-LEDs.

2.4 Device fabrication and characterization

QD-LEDs were fabricated on ITO-patterned glass substrates, beginning with a thorough cleaning process involving sequential sonication in acetone, isopropanol, deionized water for 20 min, 20 min, and 15 min, respectively. Then, the substrates were treated with UV-ozone for 15 min to eliminate organic residues and modify the surface properties. The substrates were then spin-coated with a solution of ZnO NPs (30 mg mL^{-1}) at 2000 rpm for 60 s and annealed at 90 °C for 30 min under N_2 conditions. The bottom DAB treatment was performed using a spin-coating method, where DAB was dropped onto the ZnO layer, allowed to cross-linkfor 2 min, and then spin-coated. Unbound DAB was removed through a rinsing process with toluene. Subsequently, CdSe/CdS/CdZnS QDs (20 mg mL^{-1}) were spin-coated onto the substrate at 4000 rpm for 60 s, followed by annealing at 90 °C for 30 min under N_2 conditions. Top DAB treatment followed a similar procedure to bottom DAB treatment, with the rinsing step using methanol. The DAB treated QD films were transferred to a high vacuum chamber for

thermal evaporation, where layers of 50 nm of TCTA, 10 nm of MoO_3, and 100 nm of Al were deposited. The current density–voltage–luminance-characteristics of QD-LEDs were characterized using a Keithley 2450 source measurment unit coupled with a Konica Minolta spectroradiometer CS-2000.

3. Results and discussion

Diamine-based alkyl ligands with a chain length of 4, referred to as DAB, were used as charge balancers, and their chemical structure is shown in Fig. 1. DAB was chosen as a charge balancer because of its compact nature and its binding affinity to various nanocrystals. Each end of the alkyl chain in DAB contains amines that bind to ZnO NPs or QDs *via* hydrogen bonding. Due to its compact structure, DAB induces strong interfacial dipoles without significantly altering the surface morphology. In addition, the short alkyl chain of DAB increases the probability of cross-linking ZnO NPs or QDs, which greatly suppresses leakage current and improves device conductivity by reducing nanocrystal-to-nanocrystal distance. These advantageous properties make DAB a universally applicable charge balancer in various types of QD-LEDs.

The fabrication process of QD-LEDs with DAB treatment is shown in Fig. 1. We fabricated the inverted structure of QD-LEDs consisting of indium tin oxide (ITO)/ZnO NPs/QDs/tris(4-carbazoyl-9-ylphenyl) amine (TCTA)/molybdenum trioxide (MoO_3)/aluminum (Al). To simultaneously modulate the injection rates of both electrons and holes, DAB was applied to both the electron and hole transporting sides in QD-LEDs. The first DAB treatment was conducted after the formation of ZnO films followed by QD deposition. Then, a second DAB treatment was performed on top of the QD EML. The DAB treatment was performed simply by spin coating, followed by a washing step with a neat solvent (either toluene or methanol) to remove unbound ligands from the surface. During the DAB treatment processes, some of the nanocrystals (either ZnO NPs or QDs) are cross-linked with each other, which imparts robustness to the films. Sequential thermal evaporation of TCTA, MoO_3, and Al was performed to complete the fabrication of QD-LEDs. The negligible effect on the surface morphology of ZnO and QD films with DAB treatment was confirmed by atomic force microscopy (AFM) measurements, which revealed a change in root mean square (RMS) roughness of 0.01 nm and 0.1 nm, respectively (Fig. 2(a)).

As discussed above, the standard structure for QD-LEDs based on organic/inorganic hybrid CTLs suffers from a severe charge imbalance within QD EML. The electron injection from the ZnO ETL typically exceeds the hole injection from the organic HTLs, thereby triggering the nonradiative Auger decay pathway. This process significantly degrades the luminescence efficiency of QD-LEDs, especially at high current density, and also limits the device lifetime as non-radiative recombination generates excessive heat within the device. Therefore, achieving balanced electron and hole injection rates is a prerequisite for achieving high performance and highly stable QD-LEDs. Simultaneous modification of both electron and hole injection rates in a manner that suppresses electron injection while boosting hole injection is necessary, and the application of DAB on both sides of QD EML can accomplish this.

In order to understand the changes in electron and hole injection characteristics induced by DAB treatment, we performed the ultraviolet photoelectron spectroscopy (UPS) measurements on ZnO and QD films before and after DAB treatment. In the cutoff region of the UPS measurements, the work function (ϕ) of a material can be determined according to the following equation:

$$\phi = h\nu - (E_{\text{cutoff}} - E_{\text{F}}) \quad (1)$$

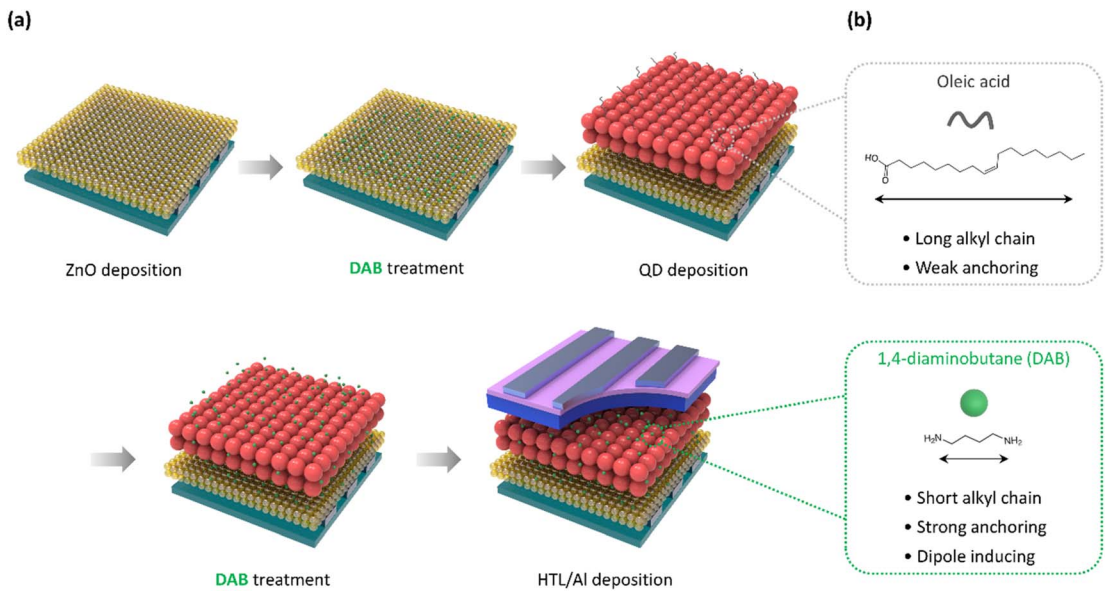

Fig. 1 Schematic illustrations of (a) the fabrication process of QD-LEDs with DAB treatment and (b) chemical structures of native oleic acid ligands and DAB.

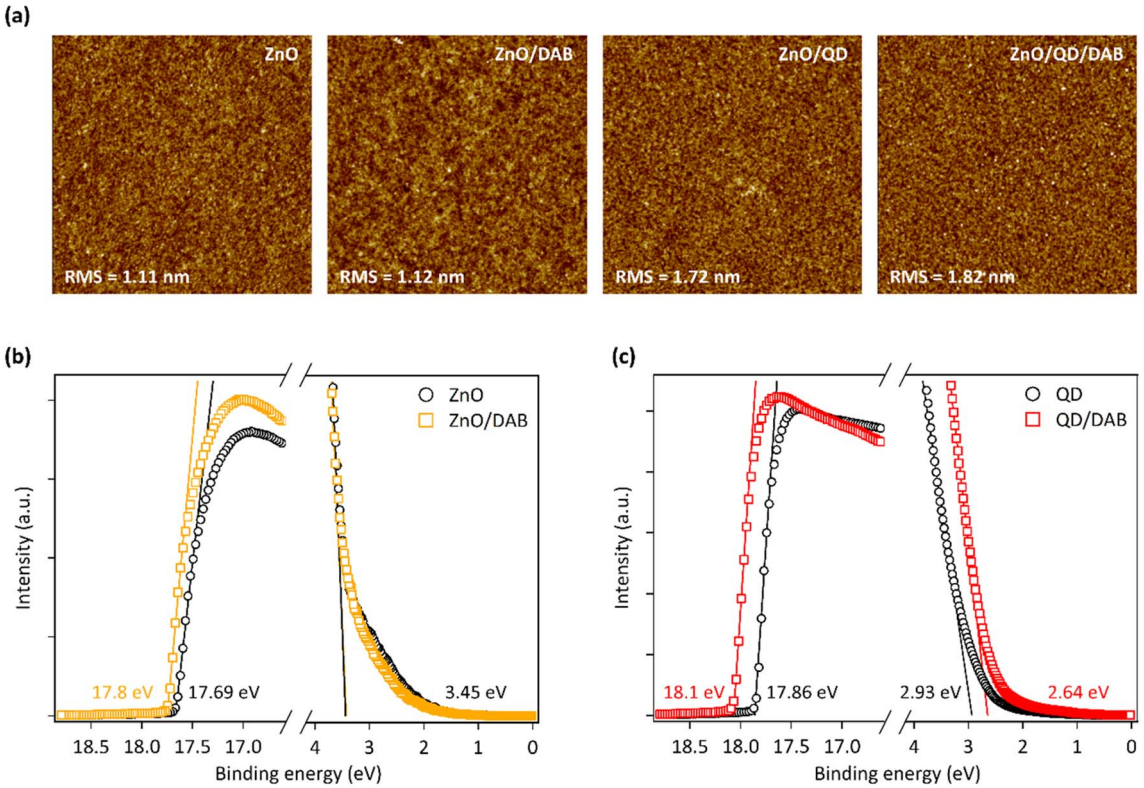

Fig. 2 (a) Atomic force microscopy (AFM) images of ZnO film, ZnO film with DAB treatment, QD film and QD film with DAB treatment (5 μm × 5 μm). Ultraviolet photoelectron spectroscopy (UPS) spectra of (b) ZnO and (c) QD films with and without DAB treatment.

where $h\nu$ is the photon energy, E_{cutoff} is the secondary electron cutoff energy, and E_F is the Fermi energy. The relative position of the valence band maximum with respect to the Fermi energy (*i.e.*, $E_F - E_{VBM}$) can be obtained from the onset energy in the Fermi edge region of the UPS measurements, and the valence band maximum energy (E_{VBM}) can be calculated by adding the work function. Fig. 2(b and c) show the changes in the UPS spectra of ZnO and QD after DAB treatment, respectively. The E_{VBM} of ZnO was shifted from −7.37 eV to −7.1 eV with DAB treatment, indicating that the overall upshift in the energy bands of ZnO due to DAB treatment. This results in an additional electron injection barrier between ZnO and QDs, which favorably suppresses electron injection rates in QD-LEDs. Similarly, the E_{VBM} of QDs was upshifted by 0.53 eV by DAB treatment, aligning the energy bands of QDs more favorably with organic HTLs.

To verify the effect of the energy band shift of ZnO and QDs induced by DAB treatment on the charge injection efficiency, we fabricated single carrier devices, namely electron-only devices (EODs) and hole-only devices (HODs). Fig. 3(a and b) show the energy band diagrams of the EODs and HODs, respectively. These devices comprise the QD EML surrounded by either ETLs or HTLs, thus allowing only electron or hole conduction. Consequently, the current densities of the single carrier devices are directly related to the charge injection or transport properties of the corresponding carrier in QD-LEDs. Fig. 3(c) shows the current densities of EODs with and without DAB treatment. With DAB treatment, the EODs exhibited notably reduced current densities, indicating a deteriorated electron injection efficiency due to DAB treatment. The reduction in current densities by DAB treatment is partly attributed to the insulating property of DAB, which prevents spontaneous electron injection from ZnO into QDs. Moreover, the upshifted energy bands of ZnO by DAB treatment creates additional injection barriers between ZnO and QDs, thus suppressing excessive electron injection into QDs. On the other hand, the current densities of the HODs are significantly increased by DAB treatment, as shown in Fig. 3(d). This increase is mainly attributed to the upshifted energy bands of QDs by DAB treatment, which results in favorable band alignments with the organic HTL. In addition, DAB treatment on QDs partially replaces native OA ligands and cross-links QDs, which increases the device conductivity and thus contributing to the increased hole current densities. These beneficial features of DAB treatment, as represented in the single carrier devices, can be applied to QD-LEDs to simultaneously engineer electron and hole injection rates to achieve charge balance in QD-LEDs.

Finally, we fabricated inverted structure QD-LEDs composed of ITO (150 nm)/ZnO NPs (30 nm)/QDs (30 nm)/TCTA (50 nm)/MoO_3 (10 nm)/Al (100 nm), and applied DAB treatment. The DAB treatment applied only to the electron transporting side (*i.e.*, ZnO/QD interface) was referred to as 'bottom' DAB, while the DAB treatment applied only to the hole transporting side (*i.e.*, QD/TCTA interface) was referred to as 'top' DAB. Fig. 4(a

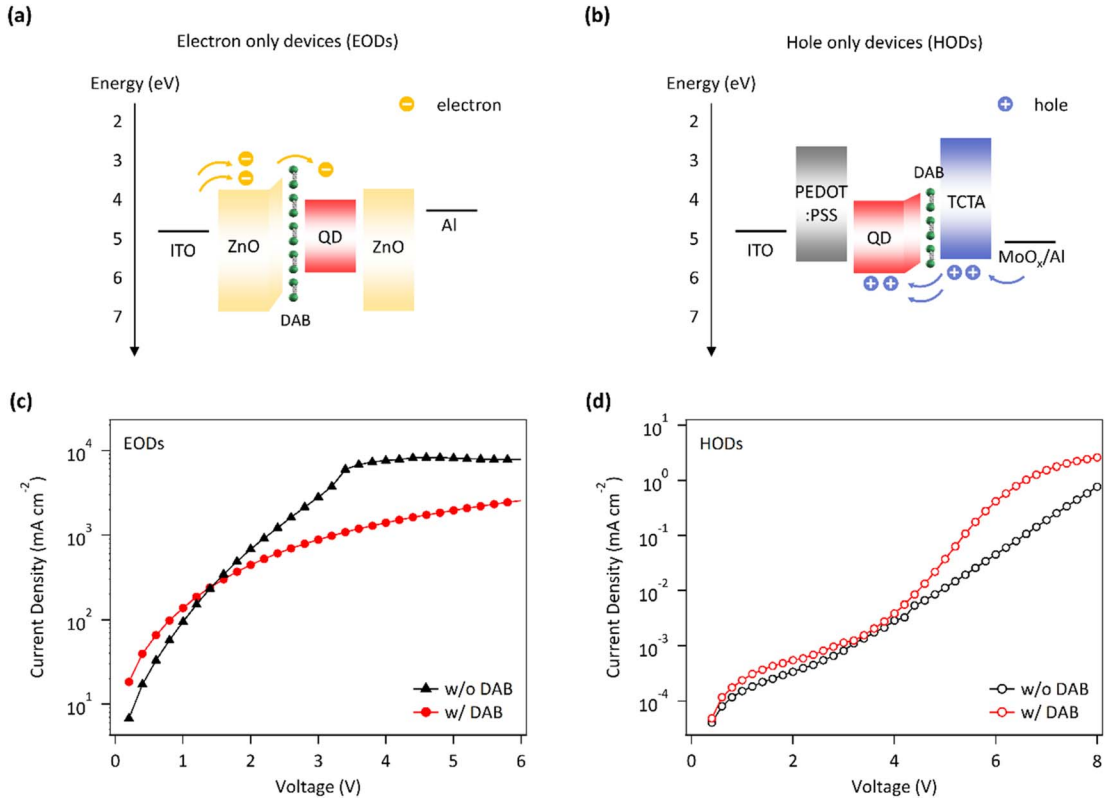

Fig. 3 Energy band diagrams of (a) electron only devices (EODs) and (b) hole only devices (HODs) with DAB treatment. The current density–voltage characteristics of (c) the EODs and (d) the HODs with and without DAB treatment.

and b) illustrates the energy band diagram of the QD-LEDs with modified electron and hole injection barriers with DAB treatment. The upshifted band structure of ZnO and QDs at the interface simultaneously modulates the injection rates of electrons and holes into the QD EMLs. Fig. 4(c) presents the EL spectra (at 6 mA cm^{-2}) of QD-LEDs with and without DAB treatment. Overall, a higher luminance was observed with DAB treatment, suggesting an improved charge balance facilitated by DAB treatment, thereby promoting efficient electroluminescence in the devices. The full width half maximum (FWHM) and emission peak wavelengths of all devices remained the same at 38 nm and 644 nm, respectively, indicating non-destructive nature of the DAB treatment (Fig. 4(c) and S1†). Fig. 4(d) and S2† shows the current density–voltage–luminance (*J*–*V*–*L*) characteristics of the QD-LEDs with and without DAB treatment, while Fig. 4(e) depicts the EQE with respect to luminance (EQE-*L*) of the corresponding devices. The QD-LEDs without DAB treatment exhibit typical *J*–*V*–*L* characteristics with a maximum EQE of 6.13%. When DAB was applied, a clear tendency in device performance was observed depending on the treatment site: when DAB was applied at the ZnO ETL-QD EML interface (bottom DAB), the current densities of the devices were reduced, while application of DAB at the QD EML and organic HTL interfaces (top DAB) resulted in increased luminance of the QD-LEDs. The reduced current densities by the bottom DAB treatment are attributed to suppressed excess electron injection from the ZnO ETL to the QD EML due to the increased interfacial barrier by the DAB treatment. The increased luminance of QD-LEDs with top DAB treatment could be attributed to the improved charge balance due to boosted hole injection and the improved QD film robustness through cross-linking. As a result, the QD-LED with bottom or top DAB treatment showed increased maximum EQE of 7.56% and 7.72%, respectively. When DAB was applied symmetrically below and above the QD-EML, the QD-LEDs exhibited both characteristics of the bottom and top DAB-treated devices, with reduced current densities and increased luminance. This led to a notably improved maximum EQE of 9.47%, which is a 1.5 fold increase compared to the device without DAB treatment. Table 1 summarizes the performance of QD-LEDs with and without DAB treatment.

The successful adoption of DAB as a charge balancer also led to improved operational stability of QD-LEDs. We evaluated the lifetime of QD-LEDs with both bottom and top DAB treatment and compared them to the devices without DAB treatment. The lifetime was evaluated by measuring the time taken for the initial luminance to degrade to 60%. An initial luminance of 900 cd m^{-2} was applied to the QD-LEDs, and lifetime measurements were conducted in ambient air without any type of passivation or encapsulation. As shown in Fig. 5, the lifetime of QD-LEDs was remarkably increased from 1.2 hours to 5.4 hours with DAB treatment, which represents a notable improvement in the operational stability of the devices. This improvement is indicative of suppressed heat generation

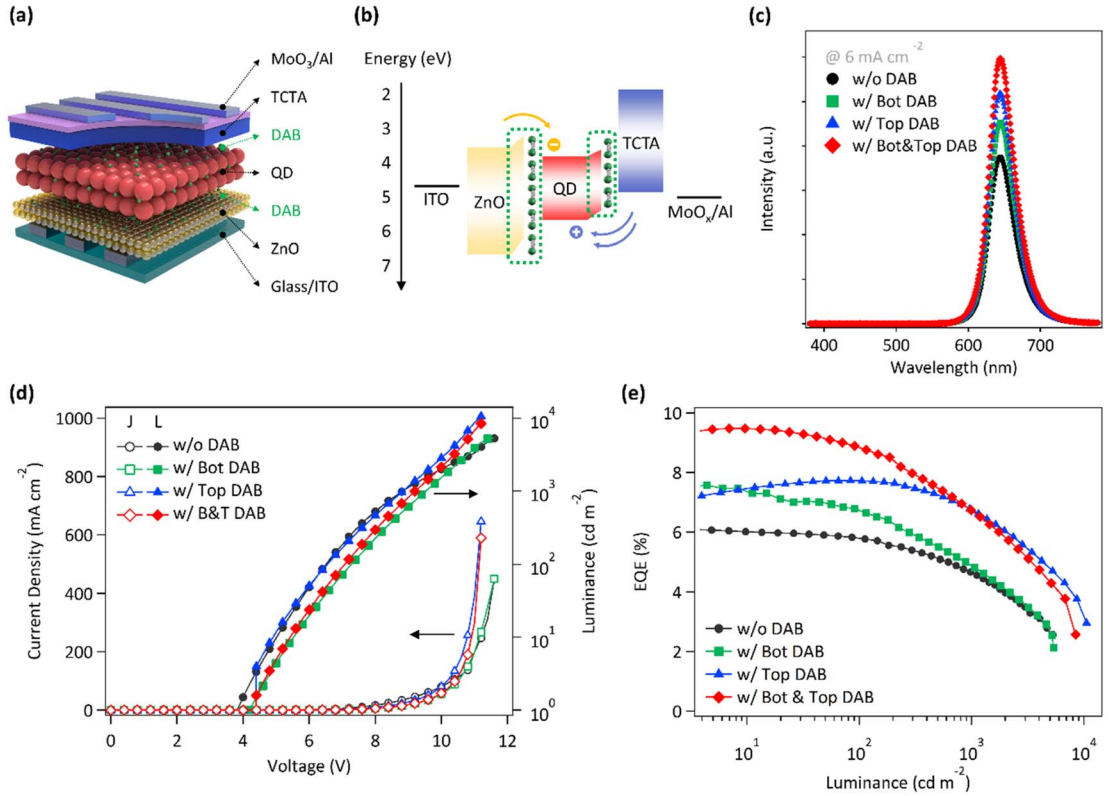

Fig. 4 (a) Device structure of QD-LEDs with DAB treatment and their (b) energy band diagram, showing suppressed electron injection with enhanced hole injection. (c) Electroluminescence (EL) intensity of the QD-LEDs with bottom and top DAB treatment (red diamond), with top DAB treatment (blue triangle), with bottom DAB treatment (green square), and without DAB treatment (black circle) at a current density of 6 mA cm^{-2}. (d) Current density–voltage–luminance (*J*–*V*–*L*) and (e) EQE-luminance characteristics of the QD-LEDs with and without DAB.

Table 1 Summary of the performance of the QD-LEDs with and without DAB treatment

	V_{on} (at 1 cd m^{-2})	Max PE (lm W^{-1})	Max CE (cd A^{-1})	Max EQE (%)
w/o DAB	3.8	3.68	4	6.13
Bottom DAB treatment	4.2	3.72	4.85	7.56
Top DAB treatment	4	3.45	5.02	7.72
Bottom and top DAB treatment	4.2	4.1	5.93	9.47

mechanisms within the QD-LEDs, such as non-radiative Auger recombination and interfacial charge accumulation caused by charge imbalance.

To verify the universality of DAB as a charge balancer, we also applied DAB treatment to conventional structure QD-LEDs consisting of ITO/PEDOT:PSS/TFB (HTL)/QDs/ZnO NPs (ETL)/Al (Fig. S3†). In the conventional structure QD-LEDs, DAB was applied only at the QD-EML and ZnO ETL interfaces to suppress excess electron injection. Similar to the case of inverted structure QD-LEDs, the *J*–*V*–*L* characteristics of DAB-treated QD-LEDs showed reduced current density and increased luminance, representing reduced excess electron injection and improved charge balance. This is mainly due to the upshift band structures of QDs by DAB treatment. Furthermore, the improved robustness of QD films by DAB treatment *via* cross-linking is beneficial in stacking with ZnO, which contributes to

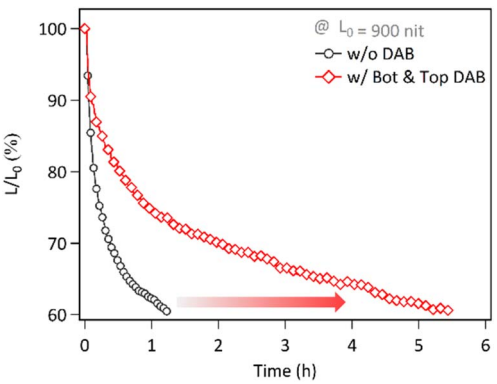

Fig. 5 Lifetime measurement of the QD-LEDs with and without DAB ligands at an initial luminance of 900 nit. The measurement was performed in ambient air without any type of passivation or encapsulation.

improved electroluminescence efficiency and stability. The QD-LEDs with DAB treatment exhibited improved maximum luminance and EQE by 1.7 times (2542 cd m^{-2} to 4329 cd m^{-2}) and 1.8 times (2.48% to 4.5%), respectively. These results indicate that DAB can be used as an efficient charge balancers regardless of the device structure, highlighting its universality. Table S1† summarizes the performance of conventional structure QD-LEDs with DAB treatment.

4. Conclusions

In conclusion, the utilization of diamine-based alkyl ligands, DAB, as a charge balancer in QD-LEDs has demonstrated significant improvements in device performance and operational stability. We have found that DAB treatment effectively modulates charge injection rates, improves charge balance, and mitigates heat generation mechanisms within the QD-LEDs. This improvement is evident across different device structures, underscoring the universality and versatility of DAB as a charge-balancing agent. The notable improvements in maximum luminance and EQE highlight the effectiveness of DAB treatment in enhancing device performance. Overall, these results not only contribute to advancing the fundamental understanding of charge transport mechanisms in QD-LEDs, but also offer promising avenues for the development of efficient and stable optoelectronic devices for diverse applications.

Data availability

The data that support the findings of this study are available from the corresponding author upon reasonable request.

Conflicts of interest

All authors declare no conflicts of interest.

Acknowledgements

This work was supported by a 2 Years Research Grant of Pusan National University.

References

1 J. Kim, J. Roh, M. Park and C. Lee, *Adv. Mater.*, 2024, 2212220.
2 J. Lee, H. Jo, M. Choi, S. Park, J. Oh, K. Lee, Y. Bae, S. Rhee and J. Roh, *Small Methods*, 2024, 2301224.
3 S. Rhee, K. Kim, J. Roh and J. Kwak, *Curr. Opt. Photonics*, 2020, **4**, 161–173.
4 M. Gao, H. Yang, H. Shen, Z. Zeng, F. Fan, B. Tang, J. Min, Y. Zhang, Q. Hua and L. S. Li, *Nano Lett.*, 2021, **21**, 7252–7260.
5 P. Yu, S. Cao, Y. Shan, Y. Bi, Y. Hu, R. Zeng, B. Zou, Y. Wang and J. Zhao, *Light: Sci. Appl.*, 2022, **11**, 162.
6 Q. Sun, Y. A. Wang, L. S. Li, D. Wang, T. Zhu, J. Xu, C. Yang and Y. Li, *Nat. Photonics*, 2007, **1**, 717–722.
7 O. Chen, J. Zhao, V. P. Chauhan, J. Cui, C. Wong, D. K. Harris, H. Wei, H.-S. Han, D. Fukumura and R. K. Jain, *Nat. Mater.*, 2013, **12**, 445–451.
8 K.-H. Lee, J.-H. Lee, W.-S. Song, H. Ko, C. Lee, J.-H. Lee and H. Yang, *ACS Nano*, 2013, **7**, 7295–7302.
9 C. Ippen, T. Greco, Y. Kim, C. Pries, J. Kim, M. S. Oh, C. J. Han and A. Wedel, *J. Soc. Inf. Disp.*, 2015, **23**, 285–293.
10 W. K. Bae, Y.-S. Park, J. Lim, D. Lee, L. A. Padilha, H. McDaniel, I. Robel, C. Lee, J. M. Pietryga and V. I. Klimov, *Nat. Commun.*, 2013, **4**, 2661.
11 S. J. Lim, M. U. Zahid, P. Le, L. Ma, D. Entenberg, A. S. Harney, J. Condeelis and A. M. Smith, *Nat. Commun.*, 2015, **6**, 8210.
12 E. Moyen, J. H. Kim, J. Kim and J. Jang, *ACS Appl. Nano Mater.*, 2020, **3**, 5203–5211.
13 H.-M. Kim, J. Kim, S.-Y. Cho and J. Jang, *ACS Appl. Mater. Interfaces*, 2017, **9**, 38678–38686.
14 M. Park, J. Roh, J. Lim, H. Lee and D. Lee, *Nanomaterials*, 2020, **10**, 726.
15 A. Alexandrov, M. Zvaigzne, D. Lypenko, I. Nabiev and P. Samokhvalov, *Sci. Rep.*, 2020, **10**, 7496.
16 M. D. Ho, D. Kim, N. Kim, S. M. Cho and H. Chae, *ACS Appl. Mater. Interfaces*, 2013, **5**, 12369–12374.
17 M. Rahmati, S. Dayneko, M. Pahlevani and Y. Shi, *Adv. Funct. Mater.*, 2019, **29**, 1906742.
18 K. Ding, H. Chen, L. Fan, B. Wang, Z. Huang, S. Zhuang, B. Hu and L. Wang, *ACS Appl. Mater. Interfaces*, 2017, **9**, 20231–20238.
19 J.-H. Kim, C.-Y. Han, K.-H. Lee, K.-S. An, W. Song, J. Kim, M. S. Oh, Y. R. Do and H. Yang, *Chem. Mater.*, 2015, **27**, 197–204.
20 Y. Lee, B. G. Jeong, H. Roh, J. Roh, J. Han, D. C. Lee, W. K. Bae, J. Y. Kim and C. Lee, *Adv. Quantum Technol.*, 2018, **1**, 1700006.
21 Q. Khan, A. Subramanian, I. Ahmed, M. Khan, A. Nathan, G. Wang, L. Wei, J. Chen, Y. Zhang and Q. Bao, *Adv. Opt. Mater.*, 2019, **7**, 1900695.
22 J. Chen, D. Song, Z. Xu, S. Zhao, B. Qiao, W. Zheng, P. Wang, X. Zheng and W. Wu, *Org. Electron.*, 2019, **75**, 105412.
23 Q. Huang, J. Pan, Y. Zhang, J. Chen, Z. Tao, C. He, K. Zhou, Y. Tu and W. Lei, *Opt. Express*, 2016, **24**, 25955–25963.
24 S. Rhee, B. G. Jeong, M. Choi, J. Lee, W. H. Jung, J. Lim and J. Roh, *ACS Photonics*, 2023, **10**, 500–507.
25 L. zur Borg, D. Lee, J. Lim, W. K. Bae, M. Park, S. Lee, C. Lee, K. Char and R. Zentel, *J. Mater. Chem. C*, 2013, **1**, 1722–1726.